

# ***Triboluminescence Results from the One Stage Light Gas Gun at the NASA Goddard Space Flight Center***

W.A. Hollerman<sup>\*</sup>, C.A. Malespin<sup>\*†</sup>, R.S. Fontenot<sup>\*</sup>, N.P. Bergeron<sup>\*††</sup>,  
R.J. Moore<sup>\*</sup>, F.T. Freund<sup>\*\*</sup>, B.W.S. Lau<sup>\*\*</sup>, P.J. Wasilewski<sup>\*\*\*</sup>, and B.M. Broussard<sup>\*</sup>

\* Department of Physics, University of Louisiana at Lafayette, Lafayette, LA 70504

\*\* NASA Ames Research Center/SETI, MS 242-4, Moffett Field, CA 94035-1000

\*\*\* NASA Goddard Space Flight Center, Astrochemistry Branch Code 691, Greenbelt, MD 20771

## **ABSTRACT**

During the summers of 2006 and 2007 work was completed to revive the one-stage gas gun located at the NASA Goddard Space Flight Center (GSFC) in Greenbelt, Maryland. This gun was last used regularly more than ten years ago and fires 63 mm (2.5 inch) diameter aluminum projectiles with masses from few grams to more than a kilogram. This renewed availability of the GSFC gun will allow us to study: 1) secondary impact events caused by hypervelocity objects, 2) energy propagation phenomenology for locations away from the actual hypervelocity impact location, and 3) impacts scenarios where a wide range of projectile masses are required. A catcher (“stripper”) was designed for the GSFC gun to stop the sabot while allowing a smaller projectile to impact a desired target at velocities up to 1 km/s. During the summer of 2006, five main tasks were completed: 1) assisted with developing a safe use checklist to fire the gun, 2) developed a methodology to reduce or mitigate all health and safety concerns, 3) developed a sample holder and sabot catcher system for small projectiles, 4) calibrated the projectile velocity with gas pressure, and 5) started collecting data for several related research projects. In 2007, triboluminescence produced by 0.3 to 0.6 km/s impacts was collected. This presentation will provide an overview into efforts to revive the gas gun at GSFC. Preliminary results into currents and associated triboluminescence generated by impacts will also be presented.

## **1. INTRODUCTION**

### **1.1 Definitions**

The generalized process of “cold light” emission is called luminescence and it refers to the absorption of energy by a material with the subsequent emission of photons. It is a phenomenon distinct from blackbody radiation, incandescence, or other such effects that cause materials to glow at high temperatures. There are various forms of luminescence, usually denoted by the method from which the electrons were excited. For example, electroluminescence happens when an electrostatic field excites the electrons, and photoluminescence is the excitation of electrons due to electromagnetic radiation. Triboluminescence (TL) is light generated from mechanical action.

Luminescent materials are sometimes called phosphors, a word invented in the early 17th century by alchemist Vincentinus Casciarolo of Bologna, Italy. Scientific research of phosphors

† Current Affiliation: Department of Physics, Auburn University, Auburn, AL 36849

†† Current Affiliation: Institute for Micromanufacturing, Louisiana Tech University, Ruston, LA 71272

dates to the 19th century using a variation of zinc sulfide type materials. Since then there have been many applications of phosphors ranging from television sets to X-ray screens.

## 1.2 Triboluminescence

The word triboluminescence comes from the Greek *tribein*, meaning "to rub," and the Latin prefix *lumen*, meaning "light". A good history and review of TL research to 1977 can be found in Walton [ref. 1]. Since then, much work has been done to characterize materials, mechanisms, and possible applications of TL. Of particular note is the work of Chandra and Zink [ref. 2] and Sweeting [ref. 3] on TL characterization and mechanisms. Recently, Sage et al. [ref. 4] and Xu et al. [ref. 5] completed research on the use of TL as a stress and damage sensor.

Triboluminescent light is a specific form of mechanoluminescence, and is the production of non-thermal, or "cold," light from any type of mechanical action or application of stress [ref. 6-10]. The mechanisms of TL light are still not fully understood, but it is believed that TL is associated with asymmetric crystal structure. Crystal bonds are broken along planes with opposing charge, and when they re-connect light is emitted as the charges pass through the separations created from the fracture. A classic example of TL light is found in the crystals used for real wintergreen flavored Lifesavers<sup>®</sup> [ref. 3]. The green/blue sparks seen when chewing the candy is TL light being emitted from the crystal breakage in the sucrose.

When a TL crystal is fractured, electrons are torn away from their parent atoms, resulting in a static discharge across the gap of the fracture. The light is emitted by several distinct, material-dependent mechanisms. The emission spectrum for sugar indicates that the light comes from the atmospheric nitrogen that fills the gap during fracture. This is the same source of light as that from lightning or touching a doorknob on a winter day. Spectra for other samples show emission characteristic of the material as well as nitrogen lines. Such spectra suggest a secondary energy process. Other substances exhibit a spectrum characteristic of the material alone. While abrupt charge separation is the same in all cases, emission mechanisms depend on material.

## 2. THEORETICAL CONSIDERATIONS

For many luminescent materials, the reduction in light intensity from the cessation of excitation can be written as:

$$I = I_0 \exp\left\{-\frac{t}{\tau}\right\}, \quad (1)$$

where:

I	=	Fluorescence light intensity (arbitrary units),
I <sub>0</sub>	=	Initial fluorescence light intensity (arbitrary units),
t	=	Time since cessation of excitation source (s), and
τ	=	Prompt fluorescence decay time (s).

The time needed to reduce the light intensity to  $e^{-1}$  (36.8%) of its original value is defined as the prompt fluorescence decay time ( $\tau$ ). Luminescence can be divided into two groups: fluorescence and phosphorescence. Phosphorescence, also known as delayed emission, has a much longer decay lifetime than fluorescence. Typical phosphorescence lifetimes can vary from 100 ms up to many seconds in duration, while the lifetimes of fluorescent materials usually range from 1 ns to

10 ms. More specifically, phosphorescence is the emission of light from a triplet excited state, which is where the electron in the ground state and excited state has the same spin orientation. The triplet state is due to the fact that the spin flips take more time to complete. Fluorescence occurs in singlet states, with the excited electron having the opposite spin of the paired ground state, resulting in a short emission time for photons. The fluorescence decay time is unique to each material. It might be possible to use the fluorescence decay time as an indicator to gauge the production of TL from impacts. For this reason, it was decided to use the decay time as the figure of merit in our attempt to detect TL from lab-generated impacts. The PI successfully used this technique to detect TL from hypervelocity impacts from 2004 to 2006 [ref. 9-10].

### 3. PRELIMINARY RESEARCH

For the last few years, the PI has been investigating the fluorescence properties of ZnS:Mn [ref. 6-10]. When excited, ZnS:Mn emits bright yellow light with a broad emission peak centered at 585 nm and a full width at half maximum (FWHM) of 65 nm. ZnS:Mn is strongly triboluminescent with a prompt fluorescence decay time of about 300  $\mu$ s. Since the decay time is unique to the material, it should be easier to observe and separate TL from other light sources, such as the impact flash.

In order to determine what phosphors emit TL light, a simple drop tower was used for testing. Figure 1 shows a picture of the drop tower that consisted of a sample tray, a 1.22 m long tube, and a Thor Labs DET10C photodiode connected to a Tektronix model TDS-1012 model oscilloscope. The phosphor powder sample was placed in the sample tray, and the tube was mounted on top of the tray with a release pin placed through one of several holes in the tube to vary the drop height. These tests were easily reproducible and multiple drops were done to reduce the random error of powder loss and drop height variation. Preliminary tests were done visually on nine different powders, shown in Table 1. These showed that a wide variety of materials produce a visible quantity of TL light at a velocity of a few meters per second, making them candidates for use on higher speed impacts.

Figure 2 shows an example TL output using the drop tower. A steel ball bearing was dropped on a small pile of ZnS:Mn powder with an impact speed of a few meters per second. The ZnS:Mn powder has an average grain size of less than 10  $\mu$ m. It has a hexagonal crystal structure that is considered “loose”, meaning that it gives off light with very little stress applied. ZnS:Mn can be seen emitting TL light simply by scratching it with a nail or other sharp object. Phosphors such as ZnS:Mn are usually composed of a semiconductor host and an impurity. For the ZnS:Mn TL data shown in Figure 2, manganese is the impurity, or sometimes called the dopant, in the crystal matrix. For the samples of ZnS:Mn used in this research, the manganese dopant concentration was about 4%. The dopant changes the band structure of the crystal by narrowing the energy gap between conduction and valence bands. With narrower energy gaps, transitions that emit light are more probable and this increases the opportunity for light to be emitted during excitation or de-excitation of electrons.



Figure 1. Picture of the drop tower used for low speed TL testing.

Table 1. Phosphors tested for visual inspection of TL light.

Phosphor	TL Observed?
YAG:Eu	Yes, very faint
La <sub>2</sub> O <sub>2</sub> S:Eu	Bright
Y <sub>2</sub> O <sub>3</sub> :Eu	Very bright
YVO <sub>4</sub> :Eu	Dim
YPO <sub>4</sub> :Dy:Eu	Dim white flash
YAG:Ce	Dim flash
Y <sub>3</sub> (Al,Ga) <sub>5</sub> O <sub>12</sub> :Ce	Dim
YAG:Dy	Dim flash
YAG:Tb	Dim
ZnS:Mn	Brightest tested flash

The interaction time of the ball bearing and the ZnS:Mn powder shown in Figure 2 is about 1 ms. After this time, the light intensity decays exponentially. The prompt decay time from this TL event was measured to be about 300  $\mu$ s, which is consistent with earlier data.

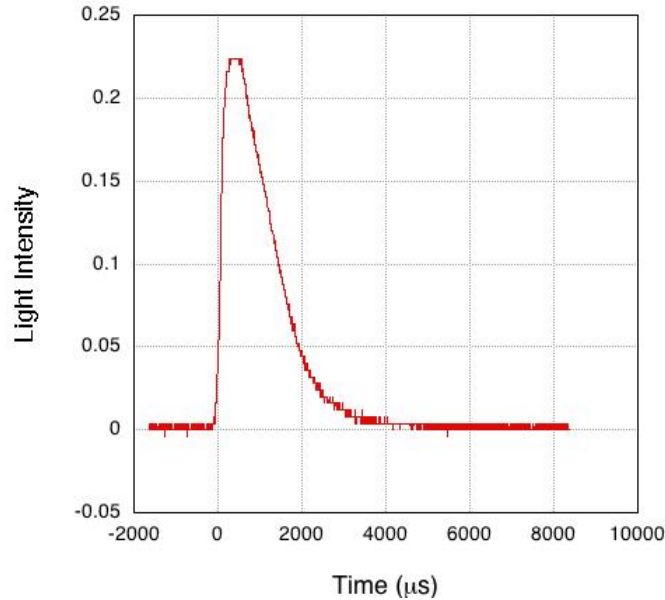


Figure 2. Light output for ZnS:Mn showing TL decay curve.

#### 4. EXPERIMENTAL HARDWARE

In April 2006, the authors were selected to participate in the NASA Exploration Systems Mission Directorate (ESMD) Faculty Student Teams summer program at the NASA Goddard Space Flight Center (GSFC). This program was designed to have a faculty and student team become involved in research with GSFC scientists and engineers. The team was tasked to make a one-stage light gas operational after years of inactivity. The one-stage gun at GSFC can fire projectiles with masses from less than 1 g to 1.2 kg at velocities as high as 1 km/s. Though the GSFC gun cannot fire projectiles in the hypervelocity regime, its main value is to study:

- Secondary impact events caused by hypervelocity objects.
- Far-field energy propagation, such as phenomena applicable to locations away from hypervelocity impact points.
- Impacts scenarios where a wide range of projectile masses are required.

When a hypervelocity impact occurs, a shower of slower, secondary particles rain down on the surrounding landscape. This process is particularly of interest to NASA with the current emphasis on building human bases on the Moon and Mars in the next 20 to 30 years. Secondary impact events near space stations or bases will have velocities like is available with the GSFC gun, but could still pose a threat to the health and safety of the inhabitants.

Another use for the GSFC gun is to look at energy propagation phenomena for lunar or Martian materials that are away from the hypervelocity impact location. This type of research is critical to help understand how impact energies are dissipated for the development of human habitations. It will also help match observations with available computer models. Since the GSFC gun has capability of firing projectiles of a few grams to 1.2 kg, any research or engineering problem that needs a wide range of masses can easily be completed. The GSFC gun is a simple and versatile tool that has endless potential for future use.

During the ESMD program, the team completed four main tasks: 1) Assisted with developing a safe use checklist to fire the gun, 2) Developing a methodology to reduce or mitigate all health and safety concerns, 3) Developing a sample holder and sabot catcher system for small projectiles, and 4) Collecting current or potential data resulting from impacts on a several rock cores. This research showed that the GSFC gun could be used as a source of meso-velocity (0.1 to 1 km/s) projectiles for TL research.

#### 4.1 NASA GSFC Gun Description

All of the impact experiments completed during this research were conducted using the high velocity one-stage light gas gun located in room twelve of building six at the NASA GSFC in Greenbelt, Maryland. The GSFC gun is capable of launching projectiles with velocities between 0.1 and 1 km/s. There is an almost linear relation between pressure and velocity as shown in Figure 3.

After several trials it was determined that for every 10 psi change in gas pressure, there was roughly a 10 m/s change in velocity. Since the gas pressure could be increased in intervals of 10 psi, the desired firing velocity could be estimated beforehand within  $\pm 10$  m/s. This gave a very wide range of target velocities. The limiting velocity occurs around 1 km/s regardless of the applied pressure, which is due mainly to the amount of gas that can be put in the gun. At this point, the gun is connected to one bottle of gas, which limits velocity of the impact.

The gun is comprised of four main parts: breech, barrel, target chamber, and catch tank, shown in Figure 4. It should be noted that the original set-up of the GSFC gun was modified for this experiment. The original “catch tank” was used as the sample chamber. The original sample or target chamber to measure the velocity of the sabot as it passed through.

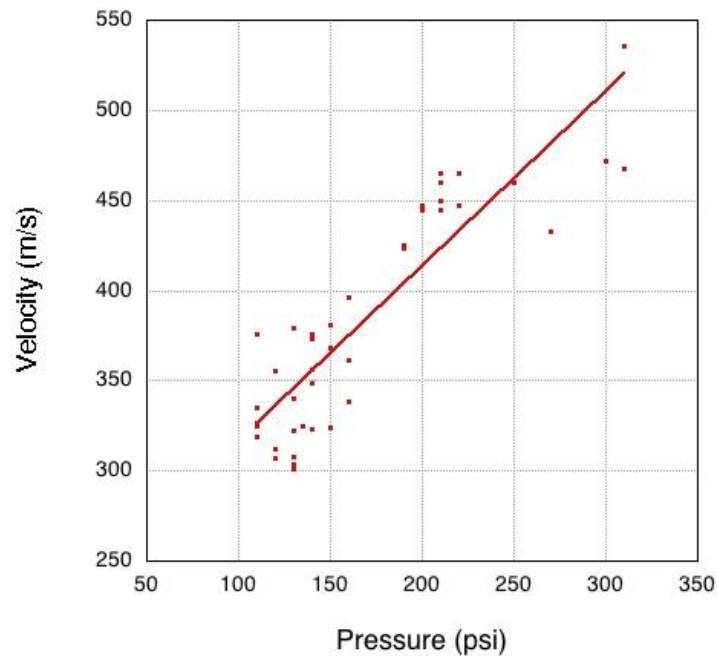


Figure 3. Velocity (m/s) versus applied breech pressure (psi) calibration graph for projectiles fired with the NSAS GSFC one-stage light gas gun.

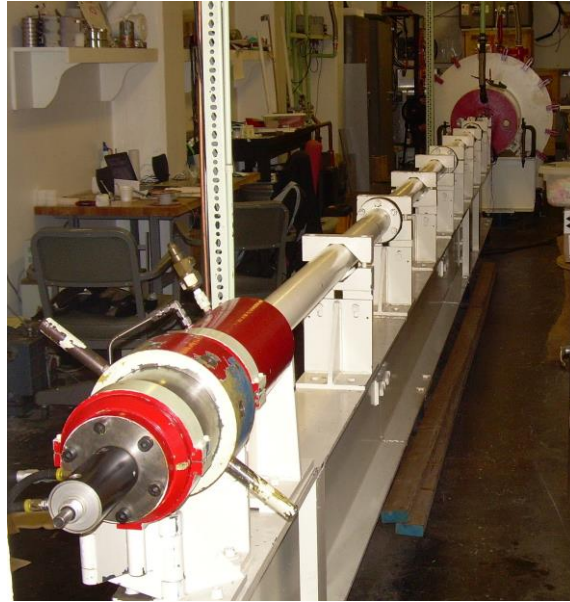


Figure 4. Picture of the one-stage light gas gun located at GSFC.

#### 4.2 Breech Chamber

The breech chamber consists of two concentric cylinders. The innermost is where the projectile is inserted and the surrounding outer cylinder where high-pressure gas, which is either helium or nitrogen, is loaded, as illustrated in Figure 5. A Teflon o-ring seals and separates the sabot. A standard mechanical pump is used to lower the pressure in the breech chamber before being fired. The helium gas is then released into the low-pressure chamber where the projectile, known as a sabot, is forced down the barrel due to the change in gas pressure as the gas expands. A second Teflon o-ring was put on the sabot and was lubricated with vacuum grease to minimize friction and heat while traveling down the gun barrel. Each sabot was made of aluminum, had a mass of approximately 90 grams, and was 6.35 cm in diameter, as shown in Figure 6.



Figure 5. Picture of the open gun breech chamber showing the firing pin on the left and the sabot loaded on the right.





Figure 6. Pictures of: A) 1.2 kg sabot, B) 90 g sabot, and C) 90 g sabot after it was shot through the catch “stripper.”

At the tip of each sabot, a piece of circular foam was cut and fitted into the opening. A small hole was cut into the center of the foam to hold a small ball bearing that would be the actual projectile hitting the target, as shown in Figure 7. Soft T-4 aluminum and clear glass balls were used as projectiles for this research. Projectiles each had a diameter of 4.7 mm.



Figure 7. Picture showing (from left): blank sabot, sabot with added foam insert, and sabot with foam insert and loaded projectile.

### 4.3 Gun Barrel and Sample Tank

The barrel of the gun, or flight tube, is 9.2 m long with the final 37 cm running inside a target chamber, or sample tank. As designed, two sets of photodiodes were used to measure the speed of the sabot in the sample tank. At the start of this research, these diodes were found to be broken. For this reason, a simple trip wire system was used to estimate the velocity of the sabot in flight. The revised speed measuring system consisted of a 1.5 V battery individually connected in series with two trip wires inside the sample tank. One trip wire ran across the tip of the barrel opening and the other wire ran across the diameter of the sample tank, at the



connection point where the catch tank and sample tank were sealed, 52 cm away from the tip of the barrel. When the sabot is fired, it breaks the two trip wires, dropping each circuit potential to zero. The second trip wire is broken slightly later in time since it is positioned 52 cm downstream from the first. Two Hewlett Packard model 54504A oscilloscopes measure the time difference between wire breaks ( $t$ ). The speed ( $s$ ) can be calculated by  $s = d/t$ , where  $d$  is 52 cm and  $t$  is the time difference when the wires are broken as measured by the oscilloscopes.

#### 4.4 Catch Tank

After passing through the sample tank, the sabot enters the “catch tank,” where the sample and detection sensors were mounted for impact. The intended target was placed in a custom built holder inside the catch tank. Figure 12 shows the two main parts: the sabot “stripper” and the actual sample holder placed some distance behind.



Figure 8. Open catch tank showing sabot catcher in front with sample mounted in back.

The purpose of the stripper was to prevent the sabot from directly impacting and damaging the sample and to minimize secondary debris impacts on the samples that could generate non-TL light. Upon impact with the stripper, the sabot was destroyed, but the ball continued through the hole to impact the sample as shown in Figure 9.



Figure 9. Picture of the metal sabot “stripper” with a sample plate and two mounted photodiode detectors facing sample.

The sabot catcher consisted of a 2.5 cm thick piece of steel that had a 2.5 cm hole cut in the center. This plate was mounted in between two pieces of angle iron. The entire set-up was bolted to a piece of wood that initially was adjustable, allowing for the catcher to be mounted closer or further from the sample depending on what the experiment required. The sabot catcher was located approximately 70 to 80 cm in front of the sample. Despite a mass of roughly 70 kg, the catcher would usually tilt and slide between 10 to 20 cm towards the sample after each shot due to the energy of the impact.

After looking at several sets of data taken with this setup, the motion of the catcher was found to generate noise in each light detector. To prevent this sliding motion, a brace was developed and implemented for the sabot catcher. The brace was constructed of aluminum pieces that were bolted together allowing the size and dimensions to be adjustable. Two “arms” ran parallel from the base of the sample table at a small angle to either side of the sabot catcher. The arms were pushed up against the back of the blue steel plates holding the sabot catcher together, which would allow them to absorb and dissipate the energy from the impact. The brace would keep the catcher from tipping over or sliding, which would reduce the amount of emitted light.

#### **4.5 Light Detection Apparatus**

Two identical photodiodes from Melles Griot were mounted on the sample table as the light collecting instruments. They were each put inside large rubber cones to reduce outside light. A large piece of quartz was then placed in front of the sensor inside the cone to be used as protection from any debris. The first detector was placed below the sample looking up at the impact area, while the second detector was mounted directly above the impact zone looking down on it. The cables for the detectors were run through PVC piping for protection against debris and out the rear in a sealed tube that came out of the catch tank and into a patch panel with 24 BNC ports. The panel wires ran to a pair of matching Melles Griot model 13Amp large dynamic range amplifiers to increase the signal. Finally, the amplifiers were each separately connected to channels one and two, for the bottom detector looking up at the sample and for the upper detector looking down respectively, of a Tektronix 2024 four channel oscilloscope.

### **5. RESULTS AND CONCLUSIONS**

TL data generated by the impact of a projectile with a target was collected at GSFC between during the summer of 2007. Approximately 200 shots were completed using the NASA GSFC gun during the course of this ESMD program. This prolific rate would not have been possible without the help and support of NASA scientists Drs. Peter Wasilewski, Friedemann Freund, and Richard Fahey.

One of these shots includes a phosphor and epoxy ball used as a projectile. The epoxy ball was made by rolling Hardman Red in ZnS:Mn and letting it harden for an hour. The ball ended up being approximately a cm wide and contained around a one-to-one mix of epoxy to phosphor.

Due to the fact that we were attempting to set the amplifier settings to the correct setting, we were only able to get one decent data shot with the epoxy phosphor ball. The last shot on July 18, 2007, was successful. This shot was fired at 320 PSI or 500 m/s into a aluminum plate with no coating that was located in a chamber that was pressurized to 1 Torr. The resulting TL decay curve is shown in Figure 10.

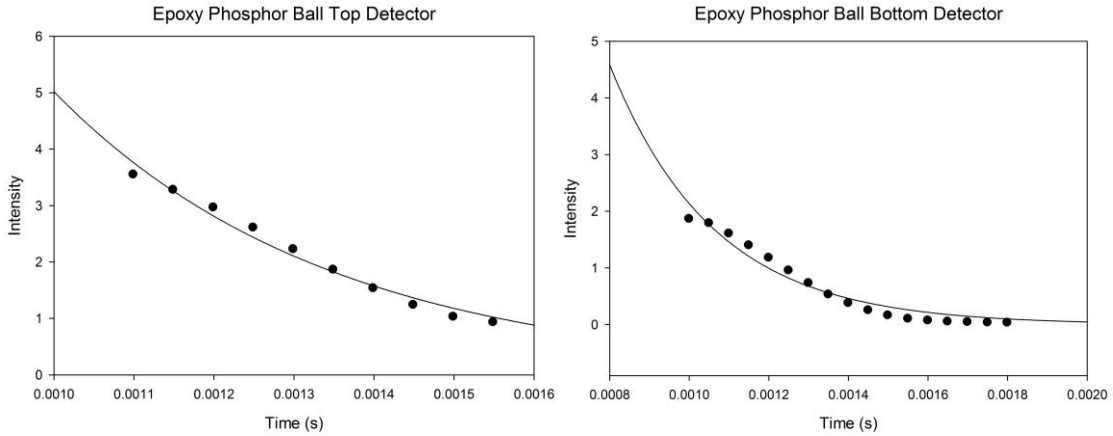


Figure 10. Epoxy Phosphor Ball Smoothed Data taken on July 18, 2007.

The slope of the decay curve using the smoothed data as shown in Figure 10 of the epoxy ball recorded by the top detector is  $2896.6374 \pm 163.5016$ . This yields a slope of  $345.228 \mu\text{s}$ . The slope of the decay curve using the smoothed data as shown in Figure 10 of the epoxy ball recorded by the bottom detector is  $3818.3189 \pm 300.8217$ . This yields a slope of  $261.895 \mu\text{s}$ . This yields an average slope of  $303.562 \pm 56.846 \mu\text{s}$ .

The reason for the smoothed data was due to the fact that we get a messy signal. At one point of the decay curve, there was a little rise and then a continued decay. At the end of the data set, there was some harmonic data. To fit this data correctly we first smoothed out the data and then started a trial and error with the exponential fit. This trial and error included deleting some of the top and end data in order to get an exponential fit that would fit the data. In the end, we got Figure 10.

## REFERENCES

1. A. J. Walton, *Advances in Physics*, 26 (6), 887-948 (1977).
2. B.P. Chandra and J.I. Zink, *J. Chem. Phys.*, vol. 73 (12), pp. 5933-5941 (1980).
3. L. Sweeting, *Chem. Mater.*, vol. 13 (3), pp. 854-870 (2001).
4. I. Sage and G. Bourhill, *Mater. Chem.*, vol. 11, pp. 231-245 (2001).
5. C.N. Xu et al., *Thin Solid Films*, vol. 352, pp. 273-277 (1999).
6. W.A. Hollerman, S.W. Allison, S.M. Goedeke, P. Boudreaux, R. Guidry, and E. Gates, *IEEE Trans. Nucl. Sci.*, vol. 50 (4), pp. 754-757 (2003).
7. F.N. Womack, N.P. Bergeron, S.M. Goedeke, W.A. Hollerman, and S.W. Allison, *IEEE Trans. Nucl. Sci.*, vol. 51 (4), pp. 1737-1741 (2004).
8. W.A. Hollerman, S.M. Goedeke, N.P. Bergeron, C.I. Muntele, S.W. Allison, and D. Ila, *Nuclear Instruments and Methods in Physics Research*, vol. B241, pp. 578-582 (2005).
9. N.P. Bergeron, W.A. Hollerman, S.M. Goedeke, M. Hovater, W. Hubbs, A. Fichum, R.J. Moore, S.W. Allison, and D.L. Edwards, *International Journal of Impact Engineering*, vol. 33 (1-12), pp. 91-99 (2006).
10. N.P. Bergeron, W.A. Hollerman, S.M. Goedeke, and R.J. Moore, "Triboluminescent Properties of Zinc Sulfide Phosphors Due to Hypervelocity Impact", *International Journal of Impact Engineering*, 2008 (Approved for publication).